

## Electrochemical Behavior of Ni-based Alloys for Hydrogen Evolution Reaction in Alkaline Media

Liliana Vazquez-Nava<sup>1</sup>, Karina Patlán-Olmedo<sup>1</sup>, Miguel A. Oliver-Tolentino<sup>2,3</sup>, Rosa Gonzalez-Huerta<sup>1</sup>, Hector J. Dorantes-Rosales<sup>4</sup>, Ariel Guzmán-Vargas<sup>4</sup> and Arturo Manzo-Robledo<sup>1,\*</sup>

<sup>1</sup>ESIQIE-IPN, Departamento de Ingeniería Química - Laboratorio de Electroquímica y Corrosión. Edif. Z-5 3er piso, UPALM, Mexico D.F. 07738, Mexico

<sup>2</sup>UPIBI-IPN, Departamento de Ciencias Básicas. Av. Acueducto s/n, Barrio La Laguna, Col. Ticomán, Mexico, D.F. 07340, Mexico

<sup>3</sup>ESIQIE-IPN, Departamento de Ingeniería Química-Laboratorio de Investigación en Materiales Porosos, Catálisis Ambiental y Química Fina, Edif. Z-5 3er piso, UPALM, Mexico D.F. 07738, Mexico

<sup>4</sup>ESIQIE-IPN, Departamento de Ingeniería en Metalurgia y Materiales. UPALM, UPALM, Mexico D.F. 07738, Mexico

Received: December 15, 2011, Accepted: February 10, 2012, Available online: April 02, 2012

**Abstract:** \*Nickel-based alloys ( $Ni_{0.8}CoO_{0.1}Zn_{0.05}MnO_{0.02}Ti_{0.01}Y_{0.01}Al_{0.01}$  (M1),  $NiO_{0.8}CoO_{0.1}Zn_{0.05}MnO_{0.02}Ti_{0.01}Y_{0.01}Al_{0.01}$  (M2) and  $NiO_{0.6}CoO_{0.35}Zn_{0.025}Ti_{0.025}$  (M3)) were synthesized from high purity powders by means of high-energy mechanical milling. The hydrogen evolution reaction (HER) kinetic-performance of the as-prepared materials was evaluated using linear sweep voltammetry at alkaline conditions and room temperature. According to kinetic parameters calculated from Tafel slopes, the sample M2 showed the better activity in the HER. These results suggest that the electrode surface state in the material play an important role in the proton-adsorption kinetic as demonstrated by SEM, open circuit potential transients and cyclic voltammetry techniques.

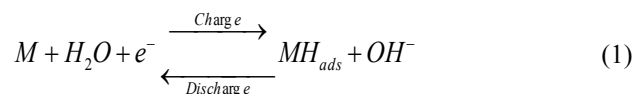
**Keywords:** Ni-based Alloys, hydrogen evolution reaction, mechanical milling, alkaline medium

### 1. INTRODUCTION

In recent years, nickel-hydride (Ni/MH) batteries have been widely used as a power source for portable electrical appliances as well as for hybrid low-emission vehicles because of their high-energy density and cleanliness [1,2]. However, the development of metal hydride (MH) electrode materials, which yield high energy per unit weight with a long charge/discharge cycle life, is a challenge for material sciences. In electrochemistry at the electrode surface, a lower exchange current density leads to a higher overpotential. A larger overpotential leads to a decrease in usable capacity and an increase in anode corrosion, and thus results in a further decrease in cycle life. Iwakura et al [3-5] have found that the high-rate discharge ability increases asymptotically with increasing exchange current density. The magnitude of the exchange current density is mainly determined by the structure of the electrodes and

the composition of the hydrogen-absorbing alloys [6], but also by the charge transfer process at the interface between the metal hydride (MH) electrode and the electrolyte. The exchange current density can also be used to derive apparent activation energy, which is a useful intrinsic parameter for evaluating the electrochemical properties of MH electrodes.

When a metal hydride electrode in an alkaline electrolyte is subjected to charging, reduction of  $H_2O$  molecule takes place producing atomic hydrogen on its surface in adsorbed states according to equation (1). Penetration of adsorbed hydrogen into the bulk of the electrode material results in the formation of metal hydride, which behaves as a reservoir of hydrogen in the rechargeable battery.



Therefore, the formation of metal hydride is an intermediate step

\*To whom correspondence should be addressed: Email: amanzor@ipn.mx  
Phone: +52 55 57296000 ext. 55146, fax +52 55 55862728

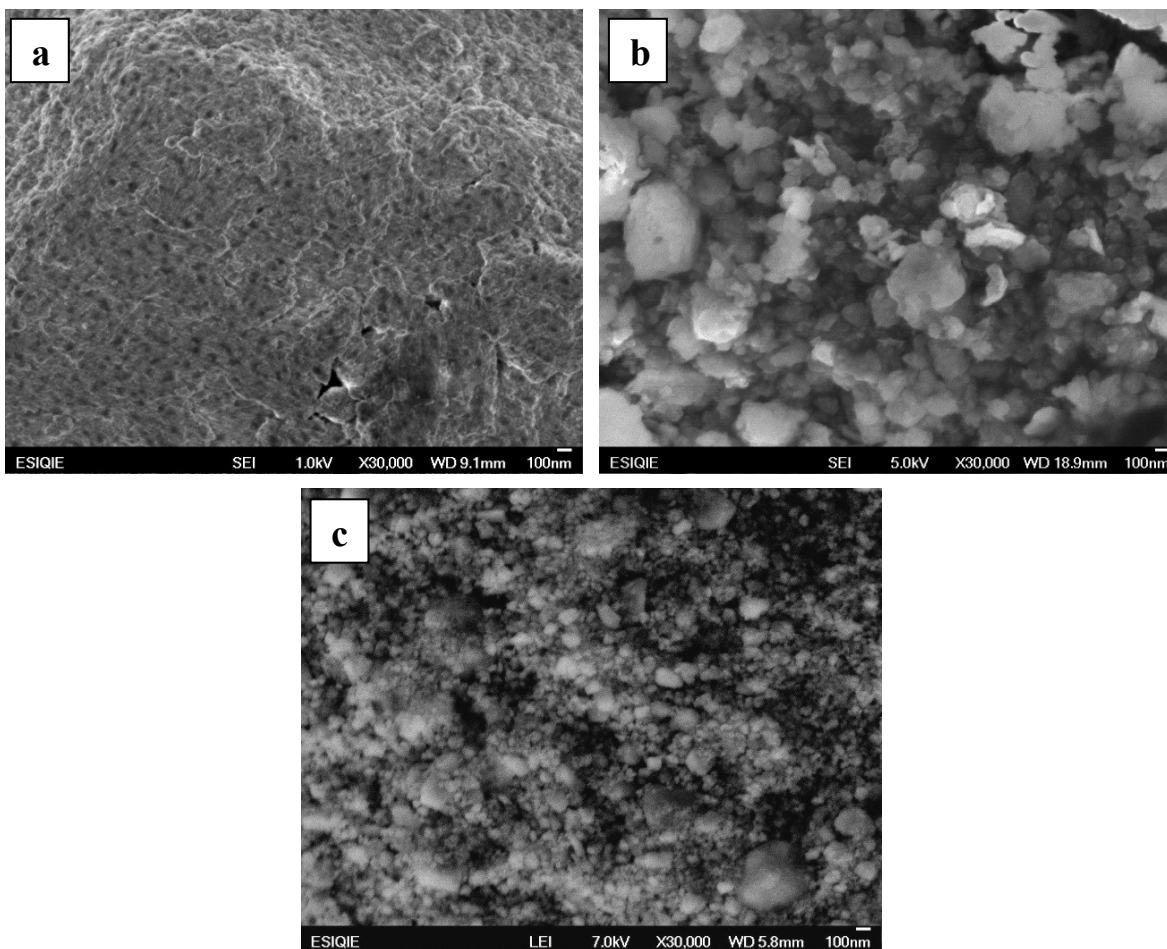


Figure 1. SEM micrographs of (a) M1, (b) M2 and (c) M3 after the milling process.

in the hydrogen evolution reaction (HER) on hydrogen-adsorbing alloys. This reaction mechanism step has been a subject of extensive investigation at various electrode materials at acid and alkaline electrolytes. In this work the electrochemical behavior of Ni-based alloys has been studied in the HER as promising materials for negative electrode in the nickel-metal hydride batteries.

## 2. EXPERIMENTAL

### 2.1. Synthesis of Materials

In this work different materials such as  $\text{Ni}_{0.8}\text{CoO}_{0.1}\text{Zn}_{0.05}\text{MnO}_{0.02}\text{-Ti}_{0.01}\text{Y}_{0.01}\text{Al}_{0.01}$ ,  $\text{NiO}_{0.8}\text{CoO}_{0.1}\text{Zn}_{0.05}\text{MnO}_{0.02}\text{Ti}_{0.01}\text{Y}_{0.01}\text{Al}_{0.01}$  and  $\text{NiO}_{0.6}\text{CoO}_{0.35}\text{Zn}_{0.025}\text{Ti}_{0.025}$  labeled as M1, M2 and M3 respectively, were obtained from high-energy mechanical milling. The raw materials were mixed in the appropriate weight ratio to obtain Ni alloys. A total amount of 7 g of the powder mixtures and 6 hardened steel balls of 12.7 mm in diameter were loaded into a steel vial; the mechanical alloying process was carried out at room temperature in an air atmosphere using a shaker mixer/mill machine. The ball-to-powder weight ratio was 7:1. To prevent excessive overheating of the vials, all experiments were carried out by means of cycles of 60 min of milling and 15 min of rest. The milling time tested was 5 h.

### 2.2. Working Electrode Preparation

The as-prepared materials were deposited on a previously polished surface (5 mm diameter) of a glassy carbon substrate (GC). The inks were prepared using 5 mg of the alloy in turn, 6  $\mu\text{L}$  Nafion (5wt %, Aldrich) and 60 mL of ethanol. The suspension was homogenized by ultrasound. Sample deposits onto the GC substrate were done with an aliquot of 5  $\mu\text{L}$  of the ink, and then dried in atmosphere of argon for 5 min.

### 2.3. Structural and morphological Characterization

The structure of milled powders was followed by X-ray diffraction (XRD) in a Bruker D8 using  $\text{Cu-K}\alpha 1$  radiation ( $\lambda = 1.542 \text{ \AA}$ , 35 kV, and 25 mA) apparatus. The morphologies of the milling powders were analyzed using a high resolution scanning electron microscopy (HRSEM), JEOL 6710.

### 2.4. Electrochemical Measurements

A three-electrode standard electrochemical cell was employed. A carbon rod and a Calomel (SCE) electrode were used as counter and reference electrodes, respectively. Prior to use, the solution was purged with argon for at least 15 min. The *i*-E characteristics were recorded in the interval from -0.1V to 0.4V/SCE. The initial poten-

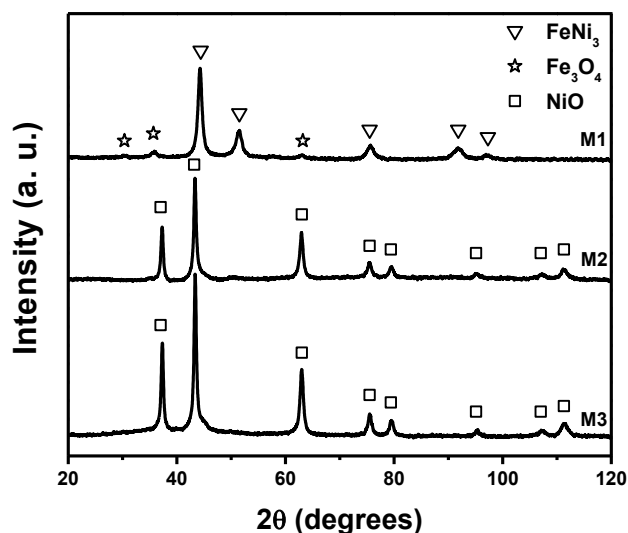


Figure 2. X-Ray Diffraction patterns for M1, M2 and M3 samples.

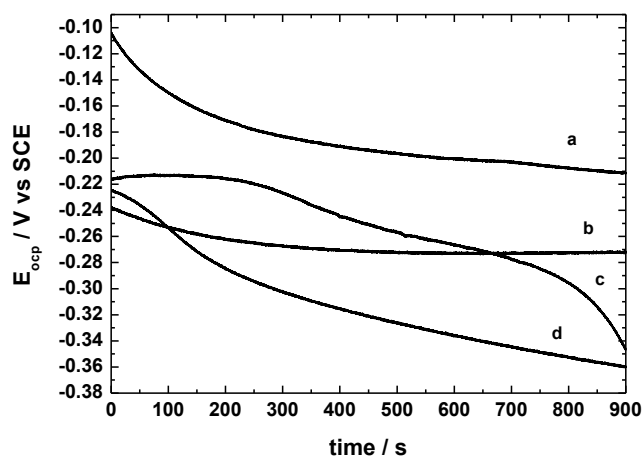


Figure 3.  $E_{ocp}$  evolution with respect to immersion time in 5 M NaOH for a) Vulcan, b) M1, c) M2, and d) M3.

tial was fixed at open circuit potential toward cathodic direction. Solution 5 M of NaOH was used as supporting electrolyte. The electrochemical experiments were done with a Potentiostat/Galvanostat (VersaSTAT 3-200).

### 3. RESULT AND DISCUSSION

#### 3.1. SEM micrographs

SEM micrographs of Ni based alloys up to 30000X are shown in Figure 1. These pictures point out that the crystallite size in M1 is lower than M2 and M3 samples. However, the particle size in the M2 and M3 are smaller than M1. The EDS analysis (figure not shown) demonstrated the presence of nickel as a main element in the alloys and the presences of Co, Zn, Mn, Ti, Y and Al in sample M1. Whereas, the presence of Co, Zn, Mn, Ti, Y and Al was evident at sample M2; and Co, Zn and Ti were found in sample M3. On the other hand, some traces of iron were found in the materials due to the ball-mechanical milling process.

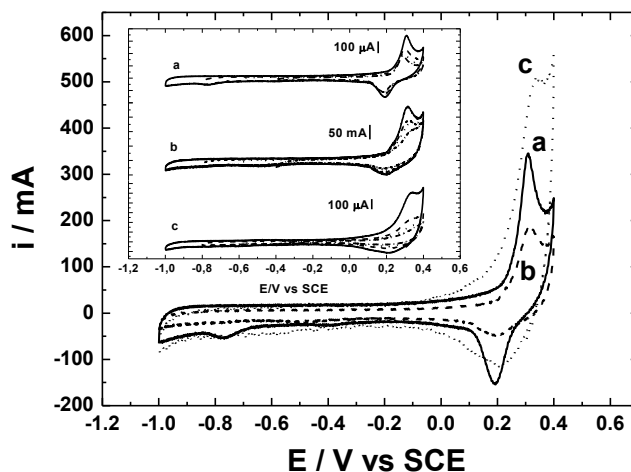


Figure 4.  $i$ - $E$  Characteristics of a) M1, b) M2, and c) M3. Inset: Cyclic Voltammetry at different inversion potentials.

#### 3.2. X- Ray Diffraction

Figure 2 shows the X-ray diffraction patterns of Ni-based alloys after the mechanical alloying process. The samples M2 and M3, exhibited the typical peak associated to the presence of NiO phase. Even as the sample M1 shows the  $FeNi_3$  and  $Fe_3O_4$  phases.

#### 3.3. Electrochemical measurement

##### 3.3.1. Open Circuit Potential

The open circuit potential ( $E_{ocp}$ ) technique is a sensitive and effective measure for monitoring spontaneous phenomena at zero current occurring at the electrode/solution interface. The  $E_{ocp}$  evolution of Ni-based alloys was monitored during 900 s (Figure 3) after immersion in a 5 M NaOH solution. These profiles were compared with the signal obtained at the carbon substrate, curve (a) in Figure 3. The  $E_{ocp}$  is more positive than the reversible potential for the HER, and also than that corresponding the thermodynamic potential related to the oxidation of Ni to NiO (i.e.  $E_{rev} = -1.16V$ ); indicating that, at the experimental conditions described here, the Ni-based alloy in turn is covered by an oxide film [7,8] protecting the electrode against further dissolution (corrosion).

##### 3.3.2. Cyclic voltammetry

Profiles  $i$ - $E$  using cyclic voltammetry (CV) were obtained for the synthesized alloys M1, M2 and M3 in a wide potential window including oxygen- and hydrogen-evolution region. Figure 4 shows the CV of nanocrystalline Ni-based alloys powders as recorded after several cycles, from OCP toward cathodic direction at scan rate of  $20 \text{ mVs}^{-1}$ . The solution was 5 M NaOH at  $25^\circ\text{C}$ . It is interesting to observe that all samples present an anodic peak attributed to the oxidation of Ni(II) to Ni(III) at c.a.  $0.35V/SCE$  [9,10]. Furthermore, the corresponding reduction peak of Ni(III) is evident at  $0.2V/SCE$ . Notice that in sample M1 (curve a) a cathodic process was found at  $-0.8V/SCE$  that can be assigned to the formation of  $\alpha\text{-Ni(OH)}_2$  [11]. On the other hand, the inset in Figure 4 illustrates the voltammetric profiles obtained at different inversion potentials ( $E_i$ ). At these conditions, the profile corresponding to sample M3 did not show redox process for Ni(III)/Ni(II) in the range from  $E_i = -0.4$  and  $-0.6 \text{ V/SCE}$ . However, when the inversion potential is

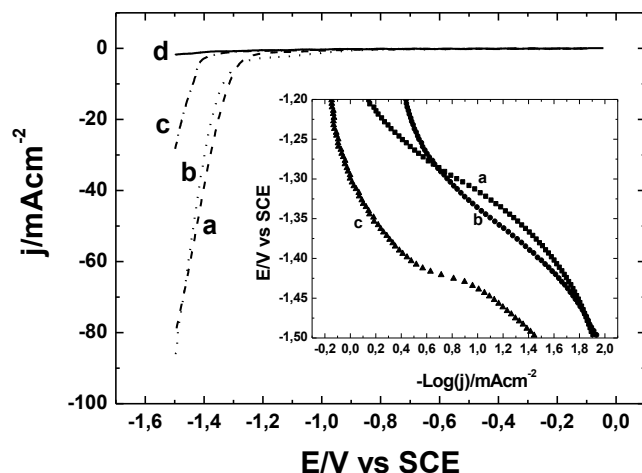


Figure 5. Linear Polarization curves for a) M1, b) M2, c) M3 and d) Vulcan. Inset: Tafel Plots.

more negative the current magnitude increases for all cases. These variations are associated with the adsorption of hydrogen during the negative-going scan, linked to the surface structure nature in the electrode material.

### 3.3.3. Electrocatalytic Activity in the HER

Linear polarization profiles of Ni-based alloys, in a solution of 5 M NaOH and at scan rate of 5 mV/s, are depicted in Figure 5. The production of hydrogen started at -1.2 V/SCE for samples M1 (curve a) and M2 (curve b). Conversely, the HER kinetic is lower for sample M3 and carbon Vulcan, see curves (c) and (d), respectively. Typical Tafel plots for the HER at milled metallic powders [10,12] are shown in the inset. Two Tafel zones are notable for samples M1 and M2 (i) at low overpotentials (from -1200 to -1350 mV/SCE) defined by a slope b1 (mV decade<sup>-1</sup>); and (ii) at high overpotential regions (from -1350 to -1500 mV/SCE) with a slope defined as b2. However, in sample M3 the Tafel slopes are situated at different region in the i-E profile: b1 in the range -1200 to -1450 mV; and b2 at -1450 to -1500 mV/SCE. Electrokinetic parameters, obtained from the inset in Figure 5, are listed in Table 1. Exchange current densities increase in the order M2>M1>M3. The better electrocatalytic performance of M2 and M1 with respect to M3 can be associated to the presence of Al, which diminishes electrode corrosion due to the formation of protective surface oxides [1]. On the other hand, the effect of yttrium might be interpreted as a synergy effect, linked to the well-known spillover process in heterogeneous catalysis, where simple cooperative functioning of the alloy components is mediated via a rapid inter-particle surface-diffusion of hydrogen adsorbed atoms [13]. A possible explanation can be

Table 1. Kinetics Parameters

	Tafel slope/mVdecade <sup>-1</sup>		Log j <sub>o</sub> /mAcm <sup>-2</sup>
	b1	b2	
M1	91.81	38.16	-6.32
M2	34.47	51.54	-3.52
M3	28.59	80.87	-8.28

due to the fact that the induced faradaic current, as the kinetic response on the external polarization, imposes spillover of the interactive dipoles and consequent changes in surface potential, which adequately exchanges the Fermi level of catalyst (alloys), and correspondingly its work function [14]. Concomitant, the presence of iron in sample M1 decreases its catalytic activity towards HER compared to sample M2.

## 4. CONCLUSION

The electrocatalytic activity of Ni-based materials obtained by mechanical alloying was evaluated in the hydrogen evolution reaction (HER) at alkaline conditions. OCP transients and CV techniques provided some clues concerning the electrode surface state in the alloys. Kinetic parameters in the HER region were determined using linear polarization. The alloy NiO<sub>0.8</sub>CoO<sub>0.1</sub>Zn<sub>0.05</sub>MnO<sub>0.02</sub>Ti<sub>0.01</sub>Y<sub>0.01</sub>Al<sub>0.01</sub> (M2) was found to yield the highest intrinsic electrocatalytic activity versus hydrogen production.

## 5. ACKNOWLEDGEMENTS

Project ICyTDF-PICS08-29 for financial support. CONACyT (160333 and 130254) and IPN (projects 20120499 and 13138) institutions. AM-R thanks Dr. Karina Suárez-Alcántara.

## REFERENCES

- [1] T. Sakai, T. Hazama, H. Miyamura, N. Kuriyama, A. Kato, H. Ishikawa, *J. Less-Common Met.*, 172, 1175 (1991).
- [2] F. Feng, D.O. Northwood, *Surf. Coatings Tech.*, 167, 263 (2003).
- [3] C. Iwakura, M. Matsuoka, K. Asai, T. Kohno, *J. Power Sources*, 38, 335 (1992).
- [4] M. Matsuoka, K. Asai, Y. Fukumoto, C. Iwakura, *J. Alloys Comp.*, 192, 149 (1993).
- [5] C. Iwakura, Y. Fukumoto, M. Matsuoka, T. Kohno, K. Shinmou, *J. Alloys Comp.*, 192, 152 (1993).
- [6] H. Kronberger, *Int. J. Hydrogen Energy*, 21, 577 (1996).
- [7] M. Metikos-Hukovic, Z. Grubac, N. Radic, A. Tonejc, *J. Mol. Catal. A-Chem.*, 249, 172 (2006).
- [8] A. Królikowski, E. Plonska, A. Ostrowski, M. Donten, Z. Stojek, *J. Solid State Electrochem.* 13, 263 (2009).
- [9] N.V. Krstajic, V.D. Jovic, Lj. Gajic-Krstajic, B.M. Jovic, A.L. Antozzi, G.N. Martelli, *Int. J. Hydrogen Energy* 33, 3676 (2008).
- [10] M.A. Oliver-Tolentino, E.M. Arce-Estrada, C.A. Cortés-Escobedo, A.M. Bolarín-Miro, F. Sánchez-De Jesús, R. de G. González-Huerta, A. Manzo-Robledo, *J. Alloys Comp.*, In press.
- [11] H. Chi-Chang, C. Chen-Yi, *J. Power Sources*, 111, 137 (2002).
- [12] K. Lian, D.W. Kirk, S. Thorpe, *Electrochim. Acta*, 36, 537 (1991).
- [13] F. Rosalbino, S. Delsante, G. Borzone, E. Angeline, *J. Alloys Comp.*, 429, 270 (2007).
- [14] J.M. Jaksic, D. Labou, C.M. Lacnjevac, A. Siokou, M.M. Jak-sic, *Applied Catalysis A: General*. 380, 1 (2010).